



NLR-TP-2000-126

Simultaneous retrieval of soil, leaf, canopy and atmospheric parameters from hyperspectral information in the red edge through model inversion

W. Verhoef



NLR-TP-2000-126

Simultaneous retrieval of soil, leaf, canopy and atmospheric parameters from hyperspectral information in the red edge through model inversion

W. Verhoef

This report is based on an article published in Proceedings Europto Series, Remote Sensing for Earth Science, and Sea Ice Applications, Florence, 20-24 September 1999, SPIE Volume 3868.

The contents of this report may be cited on condition that full credit is given to NLR and the author(s).

Division: Space
Issued: 20 March 2000
Classification of title: Unclassified



Contents

ABSTRACT	3
1. INTRODUCTION	3
2. METHODS	5
3. RESULTS	8
4. CONCLUSIONS	10
5. ACKNOWLEDGEMENTS	10
6. REFERENCES	10

2 Figures

(11 pages in total)



Simultaneous retrieval of soil, leaf, canopy and atmospheric parameters from hyperspectral information in the red edge through model inversion

Wout Verhoef

National Aerospace Laboratory NLR
P.O. Box 153, 8300 AD Emmeloord, The Netherlands
e-mail: verhoef@nlr.nl

ABSTRACT

In a modelling case study it has been investigated whether it would be possible to retrieve from optical remote sensing data the (bio)physical parameters of the coupled soil-vegetation-atmosphere system that have an effect on spectral radiances detected by spaceborne sensors. For this, optical data on single leaves generated by means of the PROSPECT model have been applied in the integrated optical soil-canopy-atmosphere radiation model OSCAR. The influences of two soil parameters, two leaf parameters, four canopy parameters and three atmospheric parameters on hyperspectral directional planetary reflectances have been simulated in a model inversion experiment.

The simultaneous retrieval of the 11 parameters has been tested using classical model inversion by means of the Gauss-Newton method of non-linear least squares parameter estimation. Preliminary results indicate that this approach has some potential, as in a number of widely differing cases the retrieval of all model parameters from 10 nm resolution hyperspectral red edge planetary reflectance data under five directions was successful.

Keywords: bidirectional reflectance, vegetation canopies, SAIL, PROSPECT, model inversion, Gauss-Newton, parameter retrieval, biophysical parameters, atmosphere, hyperspectral data

1. INTRODUCTION

The estimation of biophysical parameters of vegetation canopies from optical remote sensing data is very important for the study of land surface processes. Traditionally, this has been realised mostly by means of spectral indices, e.g. the normalised difference vegetation index (NDVI), which is derived from spectral reflectances or radiances in the near infrared and red parts of the spectrum. Spectral indices have the advantage that they can be applied very easily and that they sometimes have a fairly high correlation with a surface parameter such as fractional vegetation cover. However, the spectral reflectance of vegetation canopies is influenced by many factors simultaneously, so it is not very likely that one can obtain a good relationship between a spectral index and a single variable when other parameters vary at the same time.

In the previous SASSIS study¹ it was shown by means of model simulations that canopy LAI might be retrieved from multiple linear regression equations based on TOA multispectral (i.e. seven bands) radiance observations under five different viewing directions at an accuracy of about 12%. In this study, most variations found in reality were included, such as variation of soil type, leaf type, canopy structure, solar zenith angle and atmospheric conditions. However, it is known that the relations between surface parameters and spectral radiances are non-linear, so better retrieval results should be possible when taking these non-linear relationships into account.

The reason that the red and the near infrared are used so often to map green vegetation is that the absorption of radiation in a green leaf canopy is so different in both wavelength regions. In the red there is a strong absorption due to chlorophyll in the leaves, whereas in the near infrared there is almost no absorption at all. When the leaves are green, this great difference in absorption leads to a strong spectral response due to variation of LAI over a spectrally nearly flat soil background. This behaviour is the basis under any red – near infrared vegetation index. However, what would happen if the leaves turned yellow due to chlorophyll demolition? In that case there would be a strong spectral response as well, but it might easily be mistaken for a large decrease in canopy LAI.



From radiative transfer theory it is known that the relation between a quantity called infinite reflectance and the single scattering albedo of the medium is highly non-linear. The single scattering albedo is one minus the fraction of the intercepted radiation that is absorbed, so the absorption coefficient of the material also has a non-linear influence on the reflectance. This also holds when the optical thickness of the medium is less than infinite. For weak absorption we see an almost linear relationship between optical thickness and reflectance, whereas for strong absorption this relationship is strongly (negative) exponential. Altogether, this means that in a region where the absorption coefficient varies significantly with wavelength, the shape of the spectral reflectance curve will change with the optical thickness. In other words, when the reflectance at two wavelengths is given, the reflectance at a wavelength halfway between the first two will contain additional information, because the shape of the spectrum changes with optical thickness, even if the absorption coefficient varies linearly in the interval. This is a strong motivation to the need for high spectral resolution in certain wavelength regions. For leaf canopies the above effects come to expression as follows:

- When the leaf chlorophyll concentration decreases, this is first noticed at the wavelengths where chlorophyll absorption is weakest, i.e. in the red edge close to the near infrared and in the green. Only when it decreases much further, an effect in the red becomes visible. In the actual near infrared nothing will change in the canopy reflectance, however, as there is no sensitivity to leaf chlorophyll in that part of the spectrum.
- When the canopy LAI decreases from a high value at high leaf chlorophyll concentration, it is first noticed in the near infrared, because leaf absorption is minimum there. When LAI is low, sensitivity to LAI changes is greatest in the red.

This is also demonstrated in Fig.1, which shows the modelled canopy reflectance times 10000 in the red edge for a series of combinations of LAI and leaf chlorophyll concentration. The LAI varies according to the series 0, 0.25, 0.5, 1, 2, 4 and 8. Chlorophyll concentration is given by the series 15, 20, 25, ..., 60, 70 and 80 $\mu\text{g} / \text{cm}^2$. The spectral bands represent the wavelength range from 670 to 800 nm at 10 nm intervals.

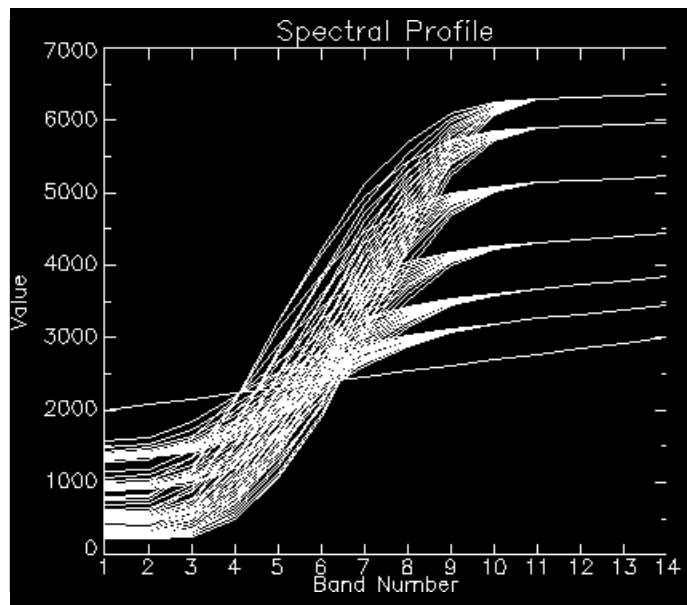


Fig.1 Effects of leaf chlorophyll and LAI on canopy reflectance in the red edge

The position of the red edge point clearly moves to longer wavelengths for higher chlorophyll contents, but the canopy LAI complicates this simple relationship, and incorporation of other parameters would complicate it even more. It can be concluded that leaf chlorophyll concentration and canopy LAI act in



different ways on spectra of the vegetation canopy reflectance in the red edge region. Due to this, it should also be possible to retrieve both parameters from high resolution spectral reflectance data in this region. Note, that with spectral reflectance data from red and near infrared alone this is not possible: several combinations of leaf chlorophyll concentration and canopy LAI can give the same combination of red and near infrared reflectance, so it would be impossible to retrieve both parameters from spectral data in the red and near infrared alone. However, hyperspectral data from the red edge region not only tell us the reflectance at both ends, but also the shape of the curve in between, and this enables us to retrieve both parameters. There have been numerous studies on the use of the red edge point (the wavelength where the first spectral derivative is maximum) as an indicator for LAI and other vegetation parameters and on how the red edge point can be derived best from hyperspectral data ^{2, 3, 4, 5, 6}. However, the red edge position has the same disadvantage as the NDVI, namely that it responds to several parameters simultaneously, so that no single one can be retrieved accurately, unless all other ones are constant, which of course is not very likely.

The red edge spectral region (670 – 800 nm) is very suitable for information on leaf chlorophyll, as in this region the chlorophyll absorption coefficient varies from very high to zero, so a large dynamic range is traversed in a relatively short wavelength interval. Also, few other optical parameters vary in this range, and the ones that do, vary only little. Therefore this region was chosen as the spectral interval of the model inversion experiment.

While leaf chlorophyll concentration and canopy LAI may be the most interesting biophysical parameters to be retrieved from remote sensing data, in reality other canopy parameters, leaf parameters, soil parameters, and atmospheric properties are expected to vary as well and are having an influence on spectral reflectances, so for some degree of realism these should also be considered in the numerical experiment.

2. METHODS

Model inversion experiments with several canopy reflectance models have already been carried out since the work of Goel and Thompson ^{10, 11} in 1984. In most of these experiments the model is called iteratively and a merit function is defined which indicates the squared distance to the solution and in which sometimes a penalty function is incorporated to avoid the exceeding of parameter boundaries. The iteration stops when the model outputs match with measured spectral data (Fig.2).

Parameter retrieval by model inversion

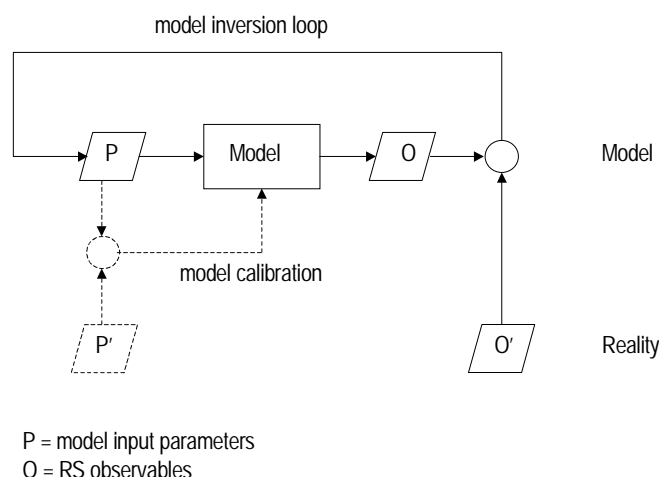


Fig.2 Model inversion loop and model calibration based on measured parameters



Models can be calibrated (dashed lines) if measured observables and parameters are both available. In the case of many output parameters, such as with hyperspectral and multidirectional data, the single quadratic merit function is formed out of information from a large number of “channels”. In this approach, the model inversion algorithm has to get its information on how to change the parameters in the direction of a solution from the Hessian, the matrix of second order partial derivatives of the merit function with respect to the parameters. As in this method all squared deviations from the target pattern are added up to form the merit function, information on how to improve the fit in a subspace of the patterns is lost. Therefore, in this section an alternative is proposed, the well-known Gauss-Newton method. Here the information on how to change the parameters in the right direction is derived from the Jacobian, which is the matrix of first partial derivatives of all model output variables with respect to the input parameters. It will be clear that in this case much more information on how to change the parameters is directly available. Therefore, this method is preferred. This method proceeds as follows:

Let the Jacobian matrix \mathbf{J} be defined by

$$\Delta \mathbf{r} = \mathbf{J} \Delta \mathbf{p},$$

where $\Delta \mathbf{p}$ is a small change in the parameter vector, and $\Delta \mathbf{r}$ the change in the vector of spectral-directional reflectances, then multiplication by the transposed of \mathbf{J} gives

$$\mathbf{J}^T \Delta \mathbf{r} = \mathbf{J}^T \mathbf{J} \Delta \mathbf{p}, \quad \text{or}$$

$$\Delta \mathbf{p} = (\mathbf{J}^T \mathbf{J})^{-1} \mathbf{J}^T \Delta \mathbf{r}.$$

The numerical stability of the Gauss-Newton method can greatly be improved by means of the Levenberg-Marquardt algorithm, which is based on the modified equation

$$\Delta \mathbf{p} = (\mathbf{J}^T \mathbf{J} + \mu \mathbf{I})^{-1} \mathbf{J}^T \Delta \mathbf{r},$$

where μ is a scalar parameter that is used to control the numerical behaviour of the algorithm. When this parameter is high, the conversion to the solution follows the steepest descent direction and therefore is secure but slow. When it is low, the Gauss-Newton direction is approximately followed, which is fast in the neighbourhood of the final solution, but unstable and possibly slow otherwise. Therefore one usually starts with a high value of the parameter, and when good progress is made, as evidenced by a decreased distance to the solution, the parameter is lowered by a certain factor. If the distance to the solution turns out to have increased, this may lead to instability, and in that case the parameter is increased in order to regain control via the steepest descent direction.

Regarding the model simulations, the following procedure was followed:

Spectra of the single leaf reflectance and transmittance in the red edge region have been simulated for a range of chlorophyll concentrations C_{ab} and 3 values of the leaf mesophyll parameter N by means of the PROSPECT model⁷. The simulations have been carried out for the wavelength range 670 – 800 nm with 10 nm steps, thus resulting in optical data at 14 wavelengths. Chlorophyll concentrations used were 15, 20, 25, 30, 35, 40, 45, 50, 55, 60, 70 and 80 $\mu\text{g}/\text{cm}^2$ (12 values) and the 3 values of the mesophyll parameter were 1.0, 1.5, and 2.0.

In a first numerical experiment, the data generated by PROSPECT were used in combination with a very simple Kubelka-Munk type canopy reflectance model in order to verify whether canopy LAI and leaf chlorophyll indeed gave different spectral responses in the red edge region. In this experiment also the soil brightness and the soil's spectral slope were varied. This enabled us to evaluate methods of compensating for soil background effects by means of first and second spectral derivatives.



In the next step the simple KM-type model was replaced by the SAILH model and a model inversion experiment was carried out in order to verify whether the most important parameters could be retrieved from hyperspectral bidirectional reflectance data. The SAILH model ⁹ is an extended version of the SAIL model ⁸ to include the hot spot effect. Here the parameters to be retrieved in the groups soil, canopy and leaf were:

Soil brightness
Soil spectral slope

Canopy LAI
Average leaf slope
Bimodality parameter of the LIDF
Canopy hot spot parameter

Leaf chlorophyll concentration
Leaf mesophyll parameter

In this experiment the solar zenith angle, the viewing zenith angle and the relative azimuth were all held fixed and no diffuse incident light on the canopy top was assumed. During the development of the model inversion procedure several enhancements were introduced, such as transformations to the input parameters in order to avoid problems due to strong non-linearity and due to the interactions between parameters and their valid ranges.

In the last experiment the SAILH model was replaced by the OSCAR model in order to further enhance the degree of realism.

The model OSCAR (Optical Soil-Canopy-Atmosphere Radiance) ⁹ is an integrated model in which SAILH has been interfaced with the soil's reflectance and scattering in the atmosphere. The number of parameters was increased from 8 to 11 by incorporation of 3 atmospheric parameters, namely:

Visibility at sea level in km
Aerosol Ångström coefficient
Aerosol single scattering albedo

Also, in order to simulate TOA observations, the planetary reflectance was used as the remote sensing observable on which model inversion was based. As in the previous experiment it already became clear that retrieval of the LIDF parameters was the most difficult if only one direction was applied, it was decided to include more directions. For this, the five best directions for estimation of LAI from planetary reflectance data, as resulting from the SASSIS ¹ study, were chosen. These are:

Viewing zenith	Azimuth
38	120
69	120
52	90
38	0
69	180

Multiplied by the number of spectral bands this gives 70 hyperspectral-directional data points on which a model inversion can be based.

The OSCAR model allows also variation of the target surroundings for modelling of the adjacency effect ⁹, but in this experiment the optical properties of the surroundings were held constant in order to avoid too much complications.



The model input parameters and possibly their transformations are described below:

It is assumed that the soil reflectance changes linearly with wavelength in this short interval. The soil's reflectance in the interval is described by means of the parameters P_1 and P_2 , called brightness and spectral slope. They are defined by

$$P_1 = (R_{670} + R_{800}) / 2, \text{ and}$$

$$P_2 = R_{800} / R_{670},$$

where R_{670} and R_{800} are the soil's reflectance at 670 and 800 nm, respectively. From these parameters the soil's reflectance at any wavelength can always be reconstructed.

The ranges for the parameters considered during model inversion were 0 – 0.6 for P_1 and 1.0 – 1.5 for P_2 .

LAI is transformed to $P_3 = \exp(-0.2 \text{ LAI})$. This reduces non-linearity, especially in the near infrared, and the valid range becomes 0 – 1.

The LIDF parameters a and b of the SAILH model are related to average leaf slope and bimodality of the leaf inclination distribution function, respectively⁹. Both parameters can vary from –1 to 1, but not independently, as the sum of their absolute values should stay less than or equal to unity. Therefore, these parameters are transformed into:

$$P_4 = 0.5 (a + b + 1)$$

$$P_5 = 0.5 (a - b + 1)$$

These parameters both range (independently) from 0 to 1 when a and b are in the valid range.

Parameter P_6 is the hot spot parameter and it is supposed to vary between 0 and 0.5.

Parameters P_7 and P_8 are the leaf parameters, describing chlorophyll concentration and the leaf mesophyll parameter. During model inversion, care must be taken to ensure that the leaf parameters actually are integer numbers in this case, as the PROSPECT model had not been integrated into OSCAR, but rather use was made of simulation results obtained with PROSPECT for discrete cases of these parameters in an earlier stage. Therefore, P_7 is an integer from 1 to 12, and P_8 is an integer from 1 to 3. In the model inversion results discussed later, these parameters are presented as real numbers, because there the predictions of the correct parameters are shown, not the values actually used in the simulations.

The atmospheric parameter visibility V has a strongly non-linear effect on the optical properties of the atmosphere. A change from 6 to 5 km may have more effect than a change from 50 to 30 km visibility. Therefore, this parameter is replaced by

$$P_9 = \exp(-0.1 V).$$

This reduces non-linearity for the atmospheric effects and the valid range becomes 0 – 1.

The other atmospheric parameters are P_{10} , the aerosol Ångström coefficient, which is assumed to vary from –0.6 to –1.3, and P_{11} , the aerosol single scattering albedo. This parameter is assumed to vary from 0.6 to 1.0.

3. RESULTS

In this section some examples of results of model inversion are discussed. In the first example below the 11 target parameters and the associate planetary reflectances times 10000 at the 14 wavelengths and in the 5 viewing directions are shown first. In the current implementation the starting guess is always at the



centre of parameter space. This choice is shown, followed by the associate reflectance values. After this are shown in one line: the iteration count, the current sum of the squared errors, and the Levenberg-Marquardt parameter of the Gauss-Newton algorithm and this pattern is repeated for all iterations. When this result was obtained, the visibility parameter was still untransformed, so for instance the target visibility is really 15 km here.

Results of model inversion program output

0.20	1.10	0.70	0.25	0.40	0.10	10.00	2.00	15.00	-0.90	0.85	<i>target parameters</i>					
583	576	626	896	1401	2019	2726	3268	3657	3816	3880	3900	3919	3939	<i>modelled spectral data</i>		
771	760	806	1060	1529	2101	2749	3242	3597	3745	3809	3833	3857	3881	<i>14 wavelengths, 5 directions</i>		
645	636	685	953	1453	2064	2760	3292	3675	3831	3896	3916	3937	3958			
775	763	818	1124	1693	2374	3138	3716	4128	4295	4363	4385	4407	4428			
827	815	860	1112	1576	2142	2785	3276	3629	3775	3838	3861	3884	3907			
0.31	1.25	0.50	0.50	0.50	0.25	6.50	2.00	21.25	-0.95	0.80	<i>starting guess</i>					
514	506	589	942	1544	2266	3114	3799	4320	4542	4637	4670	4702	4735	<i>associate spectral data</i>		
686	674	745	1061	1603	2250	2994	3583	4025	4217	4302	4336	4369	4403			
574	565	645	997	1597	2313	3147	3817	4323	4540	4633	4667	4700	4733			
737	727	831	1273	1998	2827	3763	4501	5054	5291	5393	5431	5468	5506			
729	716	788	1104	1644	2287	3029	3616	4057	4248	4333	4366	4399	4432			
1	0.185665		1.00000E-05											<i>iteration count, distance, L-M parameter</i>		
0.38	1.37	0.70	0.27	0.50	0.02	6.93	1.41	21.04	-0.70	0.86						
624	621	686	993	1554	2231	2981	3546	3951	4131	4222	4269	4318	4366			
774	764	829	1132	1667	2302	3001	3523	3895	4059	4138	4179	4220	4261			
674	668	732	1038	1596	2266	3008	3564	3962	4138	4225	4271	4317	4363			
779	771	835	1157	1752	2460	3238	3818	4233	4415	4506	4553	4601	4650			
826	816	883	1189	1724	2356	3052	3572	3943	4106	4185	4225	4266	4307			
2	4.01375E-02		1.00000E-06													
0.29	1.30	0.69	0.15	0.53	0.07	8.33	1.84	20.76	-0.70	0.84						
588	583	654	978	1543	2212	2952	3508	3904	4070	4145	4176	4207	4239			
750	740	802	1098	1619	2236	2919	3430	3794	3948	4018	4049	4079	4110			
645	638	707	1027	1586	2246	2976	3523	3911	4075	4148	4180	4211	4242			
779	770	851	1224	1862	2596	3392	3981	4397	4571	4649	4683	4716	4750			
798	787	848	1138	1651	2259	2935	3441	3802	3954	4024	4053	4083	4113			
3	2.56181E-02		1.00000E-07													
0.20	1.32	0.71	0.23	0.42	0.09	10.42	2.06	20.03	-0.70	0.87						
575	569	622	898	1412	2040	2754	3300	3692	3854	3923	3948	3973	3998			
759	748	797	1061	1549	2141	2811	3320	3685	3837	3904	3929	3955	3981			
636	628	680	956	1468	2092	2799	3338	3726	3886	3954	3979	4004	4029			
764	754	812	1128	1709	2403	3176	3758	4173	4344	4418	4444	4471	4498			
810	798	846	1108	1590	2176	2839	3344	3707	3858	3924	3949	3974	3999			
4	1.84876E-03		1.00000E-08													
0.19	1.23	0.72	0.25	0.36	0.10	11.10	2.24	17.98	-0.70	0.86						
575	568	608	847	1322	1925	2638	3201	3616	3787	3858	3879	3901	3922			
762	750	790	1026	1479	2046	2704	3217	3593	3750	3817	3841	3865	3888			
636	628	667	907	1380	1979	2682	3236	3642	3810	3880	3902	3924	3946			
765	754	796	1066	1601	2268	3041	3644	4083	4264	4338	4362	4385	4409			
815	803	842	1076	1526	2087	2740	3250	3623	3779	3846	3869	3892	3915			
5	1.26706E-03		1.00000E-09													
0.19	1.11	0.71	0.26	0.37	0.10	10.23	2.29	15.03	-0.90	0.85						
585	578	629	899	1404	2021	2722	3257	3640	3796	3860	3879	3899	3918			
774	762	808	1062	1531	2101	2745	3234	3585	3730	3794	3817	3841	3864			
647	638	687	956	1455	2064	2755	3281	3658	3811	3875	3895	3916	3937			
776	764	819	1126	1693	2371	3128	3698	4103	4267	4335	4356	4378	4400			
830	817	863	1115	1579	2144	2783	3269	3618	3762	3824	3847	3870	3893			
6	1.35831E-04		1.00000E-10													



3. C.E. Leprieur, "Preliminary evaluations of AVIRIS airborne measurements for vegetation", 9th EARSeL Symposium, Espoo, Finland, pp.524-530, 1989.
4. G. Guyot and F. Baret, "Utilisation de la haute résolution spectrale pour suivre l'état des couverts végétaux", Proc. 4th Int. Coll. on Spectral Signatures of Objects in Rem. Sens., Aussois, France, ESA SP-287, pp. 279-286, 1988.
5. H. Bach, "Die Bestimmung hydrologischer und landwirtschaftlicher Oberflächenparameter aus hyperspektralen Fernerkundungsdaten", PhD Thesis, University of Munich, 1995.
6. H. Bach and W. Mauser, "Improvements of plant parameter estimations with hyperspectral data compared to multispectral data", *Remote Sensing of Vegetation and Sea*, SPIE Vol. 2959, pp. 59-67, 1997.
7. S. Jacquemoud and F. Baret, "PROSPECT: a model of leaf optical properties spectra", *Rem. Sens. of Env.* 34: 75-91, 1990.
8. W. Verhoef, "Light scattering by leaf layers with application to canopy reflectance modeling: the SAIL model", *Rem. Sens. of Env.* 16:125-141, 1984.
9. W. Verhoef, "Theory of radiative transfer models applied in optical remote sensing of vegetation canopies", PhD Thesis, Wageningen Agricultural University, 1998.
10. N.S. Goel and R.L. Thompson, "Inversion of vegetation canopy reflectance models. IV. Total inversion of the SAIL model", *Rem. Sens. of Env.* 15: 237-253, 1984.
11. N.S. Goel, "Models of vegetation canopy reflectance and their use in estimation of biophysical parameters from reflectance data", *Rem. Sens. Reviews* 4:1-212, 1988.